Graphene Synthesis *via* Magnetic Inductive Heating of Copper Substrates

Richard Piner,[†,#] Huifeng Li,[†,#,*] Xianghua Kong,[†] Li Tao,[‡] Iskandar N. Kholmanov,[†,§] Hengxing Ji,[†] Wi Hyoung Lee,[†,⊥] Ji Won Suk,[†] Jongpil Ye,[†,‖] Yufeng Hao,[†] Shanshan Chen,[†,¶] Carl W. Magnuson,[†] Ariel F. Ismach,[†] Deji Akinwande,[‡] and Rodney S. Ruoff[†,*]

[†]Department of Mechanical Engineering and the Materials Science and Engineering Program, The University of Texas at Austin, 1 University Station C2200, Austin, Texas 78712, United States, [‡]Microelectronics Research Center and Department of Electrical Engineering, The University of Texas at Austin, Austin, Texas 78758, United States, [§]CNR-IDASC Sensor Lab Department of Chemistry and Physics, University of Brescia, via Valotti, 9, Brescia 25133, Italy, [⊥]Department of Organic and Nano System Engineering, Konkuk University, Seoul 143-701, South Korea, [‖]Department of Materials Science and Engineering, Inha University, Incheon 402-751, South Korea, and [¶]Department of Physics, Xiamen University, Xiamen 361005, People's Republic of China. [#]These authors contributed equally to this work.

ABSTRACT Scaling graphene growth using an oven to heat large substrates becomes less energy efficient as system size is increased. We report a route to graphene synthesis in which radio frequency (RF) magnetic fields inductively heat metal foils, yielding graphene of quality comparable to or higher than that of current chemical vapor deposition techniques. RF induction heating allows for rapid temperature ramp up/down, with great potential for large scale and rapid manufacturing of graphene with much better energy efficiency. Back-gated field effect transistors on a SiO_2/Si substrate showed carrier mobility up to ~14 000 $cm^2\ V^{-1}\ s^{-1}$ measured under ambient conditions. Many advantages of RF heating are outlined, and some fundamental aspects of this approach are discussed.

KEYWORDS: CVD graphene · inductive heating

With the discovery of large area monolayer growth on the surface of copper foils, a route was opened to the synthesis of very large area graphene.[1−5] To be sure, there are still a number of challenges to produce graphene of high enough quality to be commercially important. What is the best method for very large scale processing of graphene? While large ovens exist,[6,7] heating huge volumes just to heat a thin metal foil becomes less energy efficient as system size is increased. In industry, large scale heating of metals is now routinely done *via* magnetic induction which involves a changing magnetic field that induces an electric current in any conductor within the field. At radio frequency (RF), a free-standing conductor will have small eddy currents induced on and near the metal surface, leading to Ohmic heating.[8] The metal may be heated directly, without a hot environment or the need for electrical contact as would be the case for resistively heating the foil.[9] While direct Ohmic heating of a metal foil is simple and efficient, it has a number of drawbacks. First, electrical power must be brought into the reactor chamber. Further, the electrical contacts must be cooled. The connections also mean cold spots at the ends of the foils. The result can be pyrolitic carbon deposits on the sample ends. The greatest challenge to direct heating is that the foil must be thin so that its resistance is high enough for the I^2R heating to generate the desired temperature. This makes the foil fragile. Inductive heating overcomes these challenges. It works on thicker and more robust foils and can even heat bulky parts. It also allows achieving higher temperature, even above the melting point of the metal used.

In addition to its smaller energy footprint, RF heating has a number of advantages. RF heats just the metal substrate so the reactor walls remain cool, reducing thermal breakdown of reactant gases. The rate of heating and cooling of the metal can be much faster than in an oven (typically 30 °C/s for the copper foils we have studied), allowing for better control of metal temperature and reaction conditions. The cold-wall reaction chamber can be made of quartz or glass, allowing optical measurement of substrate temperature and its distribution. The emissivity of graphene differs from copper, and

* Address correspondence to huifengli@utexas.edu, r.ruoff@mail.utexas.edu.

Received for review February 5, 2013 and accepted August 9, 2013.

10.1021/nn4031564

its growth can be directly observed. With proper coil design, a uniform temperature gradient could be created, allowing exposure to the precursors at different temperatures across the same sample at the same time. This should greatly speed up research into the effects of substrate temperature on growth. RF heating will thus be a useful research tool, and its successful use could be a critical factor in scaling graphene growth for industrial applications.

Although RF inductive heating has been used to synthesize carbon nanotubes,[10] this was done by heating a substrate supporting the catalyst particles, rather than heating the catalyst particles themselves. To test whether or not graphene would grow on RF-heated metal substrates, a special reactor was constructed (Figure 1). It consists of a vacuum pumping system, gas injection system, RF heating coil and power supply, chiller, and a reaction chamber. All components are ultrahigh-vacuum-compatible. The turbo pump and high-vacuum-compatible components ensure that the system is free of oxygen and/or water. The copper foil is inserted into a quartz tube through a gate valve at one end. Outside the tube is an RF coil that will heat only the copper foil by induction. With an optical pyrometer coupled to the RF power supply, precise control of the substrate temperature is possible. There was some concern that surface currents would interfere with the growth of graphene. However, we have found that RF-heated copper foil under conditions similar to those used in a hot-wall chemical vapor deposition (CVD) system yielded high quality monolayer graphene with outstanding field effect mobility (>10 000 cm^2 V^{-1} s^{-1} under ambient conditions).

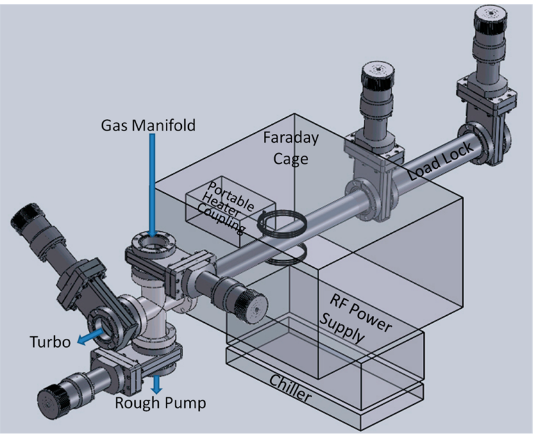

Figure 1. Apparatus design of a cold-wall reactor based on RF magnetic inductive heating. The system consists of subsystems including a vacuum pumping system, gas injection system, RF heating coils, power supply, chiller, and a reaction chamber.

RESULTS AND DISCUSSION

We grew graphene films on a 125 μm thick oxygen-free high conductivity (OFHC) copper foil. A typical synthesis process included a hydrogen annealing step, followed by an argon annealing step, and then growth under a mixture of methane and argon (see Materials and Methods for details). Each step lasts about 10 min. The copper foil can reach 1035 °C from room temperature

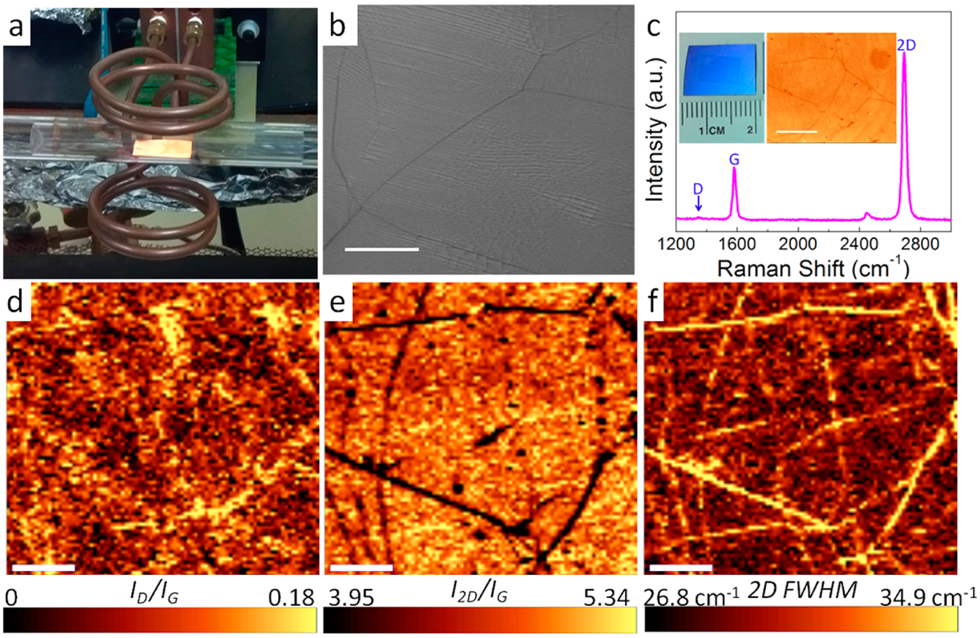

Figure 2. Photograph, SEM, and Raman characterization of RF graphene growth. (a) Photograph of a heated copper foil and RF coil. (b) SEM image of as-grown monolayer graphene on copper foil substrate, showing copper steps and graphene wrinkles. Scale bar is 3 μm. (c) Raman spectrum, G peak at 1582 cm^{-1}, 2D band at 2695 cm^{-1} (bandwidth ~30 cm^{-1}). Insets are photograph and optical microscopic image (scale bar is 20 μm) of transferred graphene on a SiO$_2$/Si substrate with 285 nm thick thermal oxide layer. (d–f) Raman mapping of transferred graphene film. (d) Intensity ratio of D band (region from 1300 to 1400 cm^{-1}) to G band (1540 to 1640 cm^{-1}), I_D/I_G. (e) Intensity ratio of 2D band (2600 to 2800 cm^{-1}) to the G band, I_{2D}/I_G. (f) Full width at half-maximum of the 2D band. Dark lines in (e) and bright lines in (f) are from wrinkles. Scale bars are 6 μm.

within 2 min, and the cooling rate is typically about 30 °C/s. Figure 2a shows the RF coil[11] used in our induction heating system and a heated copper foil inside the quartz tube. The temperature of the quartz tube (reactor wall) was monitored with an optical pyrometer, and it was always lower than 300 °C throughout the growth process. This means that it should be possible to use glass as the reactor wall. In a scanning electron microscope image of the graphene film on copper (Figure 2b), metal surface steps are readily observed, and wrinkles that cross some of the steps are obvious. This synthesized graphene was transferred with poly(methyl methacrylate) (PMMA) as a support onto a SiO_2/Si substrate with 285 nm thermal oxide, using a method similar to our previous work[12,13] (see Materials and Methods). Raman spectroscopy (WITEC Alpha 300; 488 nm laser excitation source) has been used to probe the graphene film. A typical Raman spectrum of a graphene film after transfer (Figure 2c) shows the G peak at 1582 cm^{-1} and a symmetric 2D band at 2695 cm^{-1} (bandwidth ∼30 cm^{-1}). Raman mapping in Figure 2d−f shows low I_D/I_G ratio, high I_{2D}/I_G ratio, and a 2D bandwidth in the range of 26.8−34.9 cm^{-1}, indicative of a high-quality monolayer graphene film.[14,15]

Back-gated field effect transistors (FETs) with electron-beam-evaporated Ti+Au metal contacts defined *via* a shadow mask were made to measure electrical properties. The metal contacts are 200 μm by 200 μm, with a channel length of 50, 100, and 200 μm. *I*−*V* curves were recorded on a Cascade probe station with an Agilent B1500 analyzer under ambient conditions. A widely used diffusive transport model was used for mobility extraction by fitting the total resistance of the FET device *versus* the back-gate voltage, where the contact resistance R_C, constant mobility μ, and charged impurity carrier density n_0 are the variable parameters.[16,17] Twelve devices from three growth runs were measured, and the extracted mobility was typically between 6000 and 14 000 cm^2 V^{-1} s^{-1} with a typical device with electron−hole symmetry featuring a mobility of ∼11 850 cm^2 V^{-1} s^{-1} (Figure 3a). These values are much higher than mobility values for graphene films prepared by the hot-wall furnace with ambient-pressure CVD process (APCVD) and low-pressure CVD process (LPCVD), where the same kind of copper foil and FET fabrication process were employed (see Figure S1 in Supporting Information).

As described in the Materials and Methods, the methane/argon mixture was enclosed in the quartz tube reactor during the graphene growth in a "no-flow" CVD process. The annealing of the copper foil in a pure argon environment after hydrogen annealing was found to be a critical step in our experiment to grow high-quality monolayer graphene. This results in full coverage of graphene on copper with more than 99% monolayer graphene coverage (Figure 4a). The graphene film has been transferred to a glass substrate, and its transmittance has been measured to be ∼97.6% at 550 nm wavelength. Sheet resistance has been measured using the four-probe van der Pauw method, and the average sheet resistance value is about 1300 Ω/□, which is close to typical results for monolayer graphene on the SiO_2 substrate. Direct growth of graphene after hydrogen annealing under a methane/argon mixture typically yielded more adlayers on the first graphene layer and a relatively large D peak in the Raman spectrum (Figure 4b). We also found that growth in a methane/hydrogen/argon mixture also yielded adlayers and a large D peak in the Raman spectrum. Although it was reported that hydrogen facilitates graphene growth on copper foils by acting as a cocatalyst,[5,18,19] recent work reported that hydrogen could be detrimental to the growth of high-quality graphene on hydrogen-enriched evaporated copper films[20] or in an ambient-pressure CVD.[21] Copper dissolves a significant amount of hydrogen as temperature and pressure increase.[22,23] This is less problematic for thin copper foil/film (25 μm thick or less for many studies of growth of CVD graphene)[1,2,4,24−28] and low-pressure CVD growth. However, thick copper foils under higher hydrogen pressure could contain much more dissolved hydrogen that could damage a graphene film from underneath and induce defects. Thus

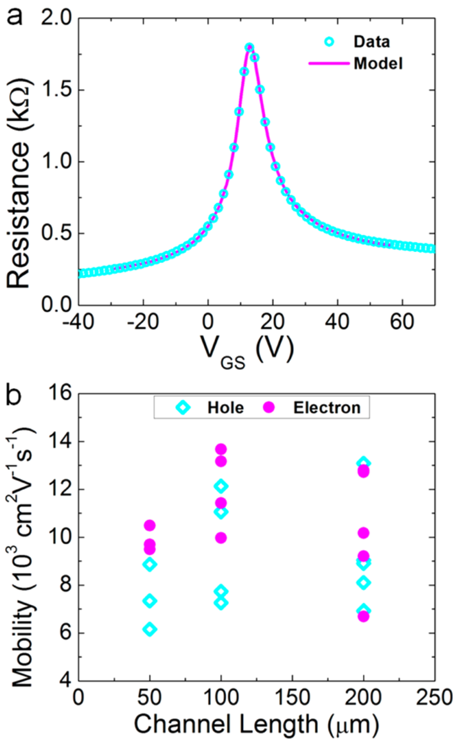

Figure 3. Electrical characterization of the RF graphene films transferred onto SiO_2/Si substrates. (a) Resistance *versus* gate voltage characteristic with a model fit for a FET device, measured under ambient conditions. Strong electron−hole symmetry was observed. The extracted carrier mobility for this device is ∼11 850 cm^2 V^{-1} s^{-1}, with the residual carrier concentration at the Dirac point of ∼2.7 × 10^{11} cm^{-2}. (b) Statistics of mobility measurement. Twelve devices were measured, and the extracted mobility is typically between 6000 and 14 000 cm^2 V^{-1} s^{-1}.

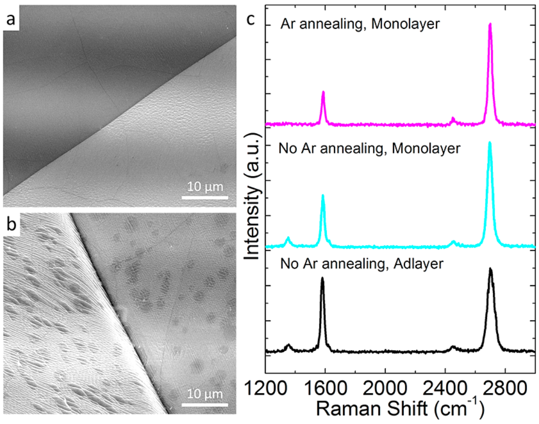

Figure 4. SEM images and Raman spectra of graphene films. (a) SEM images of graphene on copper, with argon annealing. (b) SEM images of graphene on copper, without argon annealing. (c) Raman spectra acquired on SiO_2/Si substrates for graphene films prepared with argon annealing step (top one) and without argon annealing (bottom two).

annealing the copper foil under pure argon yields a low hydrogen concentration in copper, yielding higher quality graphene growth on thicker copper foils because hydrogen is released during this annealing step.

There are a few considerations about the RF induction heating design to ensure uniform and high-quality graphene growth. (i) The typical RF coil design is a solenoid, but RF heating currents are induced perpendicular to the magnet field. For bulky materials, this is not an issue. However, in the case of a foil, the metal is almost a two-dimensional conductor. The $\vec{\mathbf{B}}$ field must be perpendicular to the surface of the foil. The copper has only limited heat conductivity, and a uniform magnetic field is required for good heating uniformity. Thus, we constructed a coil with Helmholtz-like geometry to achieve uniform and efficient heating of the foil.[11] The coils include two circular magnetic coils, each having two turns with a radius of 3.7 cm. The separation between the two coils is 7 cm. The operational frequency was typically 240 kHz. We calculated the magnetic field in the common axis direction in the copper foil plane and found that the magnitude of the magnetic field was constantly within 10% variation throughout the copper foil area. The resulting graphene was fairly uniform on the copper foil. (ii) There was also a "burn-out" problem, any thin spot of the foil will be hotter than other areas. At low pressure, this hot spot causes evaporation of copper, which causes the spot to get even hotter (a runaway process). This can be suppressed by increasing the gas pressure. (iv) The 25 μm thick copper foils had a serious "burn-out" problem, and it was very difficult to control the power to maintain the temperature at the desired set point because a thin foil has a much smaller heat capacity compared with the supporting quartz tube. By using thicker foils, both the RF coupling efficiency and the thermal stability and uniformity were greatly improved. The calculated skin depth of copper is 135 μm at room temperature and 301 μm at 1035 °C, with a RF frequency of 240 kHz. Therefore, 125 μm thickness is a good trade-off in choosing the copper foil.

CONCLUSIONS

We have demonstrated the growth of high-quality graphene films using an inductive heating cold-wall reactor, where the RF field directly heats the catalytic copper substrate. Such a heating scheme allows for rapid temperature ramp up/down, with great potential for large scale and rapid manufacturing of graphene with much better energy efficiency. Experimental studies have shown that the quality of resulting graphene is comparable to, or higher than, chemical vapor deposition techniques using hot-wall reactors.

MATERIALS AND METHODS

Graphene Synthesis. Graphene films were grown on a 125 μm thick oxygen-free high conductivity (OFHC) copper foil (C10200, Eagle Brass). This foil was cut into 1.5 cm × 3 cm strips that were cleaned using an ultrasonic system (VWR, B2500A-MT) with an acetone bath for 15 min, and then rinsed by acetone and isopropyl alcohol before being blow dried with nitrogen gas. The foil was then placed inside a 0.8 in. ID fused silica tube that was then put inside a 1 in. fused silica tube. (This makes it easy to load/unload the copper foils and clean any evaporated copper from the small diameter silica tube.) A typical process is as follows: (i) load the Cu foil into the silica tube, evacuate, fill with 5% hydrogen balanced with argon to ambient pressure, heat to 1035 °C for 10 min; (ii) evacuate and fill with pure argon to ambient pressure and heat to 1035 °C for 10 min; (iii) evacuate, fill with pure argon to 100 Torr, heat to 1035 °C, fill the chamber with 5% methane balanced with argon to 150 Torr, keep the temperature at 1035 °C for 10 min and turn off the heating power. The copper foil can reach 1035 °C from room temperature within 2 min, and the cooling rate is typically about 30 °C/s.

Graphene Transfer. The as-grown graphene films were transferred to SiO_2/Si substrates by using poly(methyl methacrylate) (PMMA; Sigma-Aldrich, MW 996K) as a supporting material. The graphene–copper foil substrate was spin-coated with PMMA at 4000 rpm for 1 min (acceleration of 500 rpm/s), followed by 90 °C heating on a hot plate for 10 min to remove toluene. The copper foil was then removed by 0.3 M ammonium persulfate (Sigma-Aldrich) solution overnight. The floating PMMA/graphene film was rinsed repeatedly using DI water (12 times) and then transferred to a pure DI water-filled Petri dish in an attempt to remove residual etchant. A SiO_2/Si substrate was brought into contact with the floating graphene–PMMA film from below and used to pull it from the surface of the water. The sample was dried in air for 30 min and then vacuum-dried for another 30 min, both at ambient temperature. It was then heated on a hot plate at 150 °C for 2 h to allow the PMMA to reflow to improve the contact between graphene and substrate. PMMA was then removed using acetone at ambient temperature.

Characterization. Scanning electron microscopy images were obtained using an FEI Quanta-600 FEG-ESEM at an accelerating voltage of 30 kV. Raman spectra were obtained using a WITec Alpha 300 confocal Raman spectroscope with a laser wavelength of 488 nm and a 100× objective lens (laser spot size is 300 nm). A Cascade probe station with an Agilent B1500 analyzer was used for electrical measurement of FET devices.

Conflict of Interest: The authors declare no competing financial interest.

Acknowledgment. We appreciate support from the W.M. Keck foundation and the NRI SWAN Center at UT-Austin.

Supporting Information Available: Carrier mobilities for RFCVD, LPCVD, and APCVD graphene; SEM, EBSD, Raman characterization for RFCVD and APCVD graphene; transmittance of RFCVD graphene; growth conditions for LPCVD and APCVD graphene. This material is available free of charge *via* the Internet at http://pubs.acs.org.

REFERENCES AND NOTES

1. Li, X.; Cai, W.; An, J.; Kim, S.; Nah, J.; Yang, D.; Piner, R.; Velamakanni, A.; Jung, I.; Tutuc, E.; *et al.* Large-Area Synthesis of High-Quality and Uniform Graphene Films on Copper Foils. *Science* **2009**, *324*, 1312–1314.
2. Li, X.; Magnuson, C. W.; Venugopal, A.; Tromp, R. M.; Hannon, J. B.; Vogel, E. M.; Colombo, L.; Ruoff, R. S. Large-Area Graphene Single Crystals Grown by Low-Pressure Chemical Vapor Deposition of Methane on Copper. *J. Am. Chem. Soc.* **2011**, *133*, 2816–2819.
3. Regmi, M.; Chisholm, M. F.; Eres, G. The Effect of Growth Parameters on the Intrinsic Properties of Large-Area Single Layer Graphene Grown by Chemical Vapor Deposition on Cu. *Carbon* **2012**, *50*, 134–141.
4. Li, X.; Magnuson, C. W.; Venugopal, A.; An, J.; Suk, J. W.; Han, B.; Borysiak, M.; Cai, W.; Velamakanni, A.; Zhu, Y.; *et al.* Graphene Films with Large Domain Size by a Two-Step Chemical Vapor Deposition Process. *Nano Lett.* **2010**, *10*, 4328–4334.
5. Mattevi, C.; Kim, H.; Chhowalla, M. A Review of Chemical Vapour Deposition of Graphene on Copper. *J. Mater. Chem.* **2011**, *21*, 3324–3334.
6. Bae, S.; Kim, H.; Lee, Y.; Xu, X.; Park, J.-S.; Zheng, Y.; Balakrishnan, J.; Lei, T.; Ri Kim, H.; Song, Y. I.; *et al.* Roll-to-Roll Production of 30-Inch Graphene Films for Transparent Electrodes. *Nat. Nanotechnol.* **2010**, *5*, 574–578.
7. Hesjedal, T. Continuous Roll-to-Roll Growth of Graphene Films by Chemical Vapor Deposition. *Appl. Phys. Lett.* **2011**, *98*, 133106-3.
8. Inan, A. S. *Engineering Electromagnetics*, 1st ed.; Prentice Hall: New York, 1998; p 800.
9. Kobayashi, T.; Bando, M.; Kimura, N.; Shimizu, K.; Kadono, K.; Umezu, N.; Miyahara, K.; Hayazaki, S.; Nagai, S.; Mizuguchi, Y.; *et al.* Production of a 100-m-Long High-Quality Graphene Transparent Conductive Film by Roll-to-Roll Chemical Vapor Deposition and Transfer Process. *Appl. Phys. Lett.* **2013**, *102*, 023112-4.
10. Sosnowchik, B. D.; Lin, L. Rapid Synthesis of Carbon Nanotubes *via* Inductive Heating. *Appl. Phys. Lett.* **2006**, *89*, 193112-3.
11. Zinn, S.; Semiatin, S. Coil Design and Fabrication: Basic Design and Modifications. *Heat Treat.* **1988**, *12*, 32–36.
12. Li, X.; Zhu, Y.; Cai, W.; Borysiak, M.; Han, B.; Chen, D.; Piner, R. D.; Colombo, L.; Ruoff, R. S. Transfer of Large-Area Graphene Films for High-Performance Transparent Conductive Electrodes. *Nano Lett.* **2009**, *9*, 4359–4363.
13. Suk, J. W.; Kitt, A.; Magnuson, C. W.; Hao, Y.; Ahmed, S.; An, J.; Swan, A. K.; Goldberg, B. B.; Ruoff, R. S. Transfer of CVD-Grown Monolayer Graphene onto Arbitrary Substrates. *ACS Nano* **2011**, *5*, 6916–6924.
14. Ferrari, A. C. Raman Spectroscopy of Graphene and Graphite: Disorder, Electron−Phonon Coupling, Doping and Nonadiabatic Effects. *Solid State Commun.* **2007**, *143*, 47–57.
15. Malard, L. M.; Pimenta, M. A.; Dresselhaus, G.; Dresselhaus, M. S. Raman Spectroscopy in Graphene. *Phys. Rep.* **2009**, *473*, 51–87.
16. Kim, S.; Nah, J.; Jo, I.; Shahrjerdi, D.; Colombo, L.; Yao, Z.; Tutuc, E.; Banerjee, S. K. Realization of a High Mobility Dual-Gated Graphene Field-Effect Transistor with Al_2O_3 Dielectric. *Appl. Phys. Lett.* **2009**, *94*, 062107-3.
17. Venugopal, A.; Chan, J.; Li, X.; Magnuson, C. W.; Kirk, W. P.; Colombo, L.; Ruoff, R. S.; Vogel, E. M. Effective Mobility of Single-Layer Graphene Transistors as a Function of Channel Dimensions. *J. Appl. Phys.* **2011**, *109*, 104511-5.
18. Vlassiouk, I.; Regmi, M.; Fulvio, P.; Dai, S.; Datskos, P.; Eres, G.; Smirnov, S. Role of Hydrogen in Chemical Vapor Deposition Growth of Large Single-Crystal Graphene. *ACS Nano* **2011**, *5*, 6069–6076.
19. Bhaviripudi, S.; Jia, X.; Dresselhaus, M. S.; Kong, J. Role of Kinetic Factors in Chemical Vapor Deposition Synthesis of Uniform Large Area Graphene Using Copper Catalyst. *Nano Lett.* **2010**, *10*, 4128–4133.
20. Tao, L.; Lee, J.; Chou, H.; Holt, M.; Ruoff, R. S.; Akinwande, D. Synthesis of High Quality Monolayer Graphene at Reduced Temperature on Hydrogen-Enriched Evaporated Copper (111) Films. *ACS Nano* **2012**, *6*, 2319–2325.
21. Gao, L.; Ren, W.; Zhao, J.; Ma, L.-P.; Chen, Z.; Cheng, H.-M. Efficient Growth of High-Quality Graphene Films on Cu Foils by Ambient Pressure Chemical Vapor Deposition. *Appl. Phys. Lett.* **2010**, *97*, 183109-3.
22. Wampler, W. R.; Schober, T.; Lengeler, B. Precipitation and Trapping of Hydrogen in Copper. *Philos. Mag.* **1976**, *34*, 129–141.
23. Shapovalov, V. In *Metal-Hydrogen Phase Diagrams in the Vicinity of Melting Temperatures*, Proceedings of the 1999 International Symposium on Liquid Metal Processing and Casting, Santa Fe, New Mexico, February 1999; pp 21−24.
24. Levendorf, M. P.; Ruiz-Vargas, C. S.; Garg, S.; Park, J. Transfer-Free Batch Fabrication of Single Layer Graphene Transistors. *Nano Lett.* **2009**, *9*, 4479–4483.
25. Lee, Y.; Bae, S.; Jang, H.; Jang, S.; Zhu, S.-E.; Sim, S. H.; Song, Y. I.; Hong, B. H.; Ahn, J.-H. Wafer-Scale Synthesis and Transfer of Graphene Films. *Nano Lett.* **2010**, *10*, 490–493.
26. Lee, Y. H.; Lee, J. H. Scalable Growth of Free-Standing Graphene Wafers with Copper (Cu) Catalyst on Sio/Si Substrate: Thermal Conductivity of the Wafers. *Appl. Phys. Lett.* **2010**, *96*, 083101.
27. Srivastava, A.; Galande, C.; Ci, L.; Song, L.; Rai, C.; Jariwala, D.; Kelly, K. F.; Ajayan, P. M. Novel Liquid Precursor-Based Facile Synthesis of Large-Area Continuous, Single, and Few-Layer Graphene Films. *Chem. Mater.* **2010**, *22*, 3457–3461.
28. Ismach, A.; Druzgalski, C.; Penwell, S.; Schwartzberg, A.; Zheng, M.; Javey, A.; Bokor, J.; Zhang, Y. Direct Chemical Vapor Deposition of Graphene on Dielectric Surfaces. *Nano Lett.* **2010**, *10*, 1542–1548.